Singular perturbations of the Holling I predator-prey system with a focus

Zegeling, André; Kooij, Robert E.

DOI
10.1016/j.jde.2020.04.011

Publication date
2020

Document Version
Final published version

Published in
Journal of Differential Equations

Available online at www.sciencedirect.com

ScienceDirect

J. Differential Equations 269 (2020) 5434–5462

Journal of Differential Equations

www.elsevier.com/locate/jde

Singular perturbations of the Holling I predator-prey system with a focus

André Zegeling [a,*], Robert E. Kooij [b]

[a] *Guilin University of Aerospace Technology, Jinji Road 2, Guilin, China*

[b] *Delft University of Technology, Faculty of Electrical Engineering, Mathematics and Computer Science, Network Architectures and Services, Mekelweg 4, 2628 CD Delft, the Netherlands*

Received 7 August 2019; revised 3 April 2020; accepted 4 April 2020

Available online 16 April 2020

Abstract

We study the occurrence of limit cyles in a model for two-species predator-prey interaction (referred to as Holling I). This model is based on the phenomenological fitting of the so-called functional response function to observed data in nature by a continuous, piecewise differentiable function. Of the original models presented by Holling it is the only model for which the possible asymptotic behaviour of the prey and predator densities has not been determined yet.

We extend the work of Liu who showed that for certain values of parameters of the Holling I system at least two nested limit cycles will occur surrounding a focus. His case corresponds to a bifurcation problem where limit cycles are created from a system with a continuum of singularities, i.e. a singular perturbation problem with slow-fast solutions.

We prove that exactly two hyperbolic limit cycles occur after perturbation.

MSC: 34C15; 92D25

Keywords: Generalized Gause model; Singular perturbation; Holling; Functional response; Limit cycles

* Corresponding author.

E-mail address: zegela1@yahoo.com (A. Zegeling).

https://doi.org/10.1016/j.jde.2020.04.011

0022-0396/

1. Introduction

1.1. Two-species predator-prey systems

One of the earliest two-species predator-prey systems with limit cycles [15] was the Gause model of the form:

$$\dot{x} \equiv \frac{dx}{dt} = h_1(x) - p(x)y, \ \dot{y} \equiv \frac{dy}{dt} = -h_2(y) + \gamma p(x)y, \tag{1.1}$$

where $x(t) \geq 0$ represents the prey density, $y(t) \geq 0$ represents the predator density, $h_1(x)$ represents the change in prey-population due to natural growth and $h_2(y)$ represents the natural death rate of the predator-population.

In this paper we consider a logistic growth rate for the prey population in the form $h_1(x) = \phi x(1 - \frac{x}{k})$, with $\phi > 0$, $k > 0$, essentially modelling that for small populations an exponential growth occurs which will saturate at level $x = k$, i.e. for larger populations the growth rate is slowing down in order not to exceed a threshold value k. We take the function $h_2(y)$ in the form $h_2(y) = \delta y$, which represents an exponential natural death rate of the predator population. The parameter γ is sometimes referred to as the conversion rate.

Of critical importance in such a model is the choice of the function $p(x)$, the functional response function representing the rate of consumption of prey per unit of predator density. The interesting feature of these functions is that most of them as discussed in the literature are differentiable functions of the underlying variable (the prey density), except for the continuous, piecewise differentiable Holling type I function which we will discuss in this paper. Our aim is to investigate what the consequences are of choosing a continuous, piecewise differentiable functional response function in modelling the interaction between predator and prey.

1.2. Functional response

The interaction between the predators and preys is determined by the functional response $p(x)$ in the Gause-model (1.1). Many different forms for $p(x)$ have been discussed in the literature (see for instance [12], [13], [17], [21], [22], [24], [28], [23], [33], [42]). For an overview, see [20].

One of the earliest choices for the functional response function was proposed by Holling [16], [17]. Its most important property is that it is monotonically increasing (or constant) as a function of x. Cases where $p(x)$ is not monotonic are typically describing a group defense effect (see [13], [18], [19], [34], [38]) which we will not discuss here. Holling introduced different functions satisyfing this monotonicity property. For the Holling types II and III of the form $p(x) = \frac{x}{c+x}$ and $p(x) = \frac{x^2}{c+x^2}$, respectively, and its extension $p(x) = \frac{x^n}{c+x^n}, c > 0, n \geq 1$, see [22], the existence and uniqueness of limit cycle in (1.1) was proved (see [2], [24]). These functional response functions have the common property that they are not only monotonically increasing but also differentiable and bounded for large x. The Holling type II has proved to be one of the more popular choices in the literature (see [20]).

In the overview paper [20] it was remarked that there are fundamentally two types of choices for the functional response function.

On one hand one could try to fit the function to data observed in a real-life biological system using some kind of parameterized function in which the parameters are chosen in an optimal

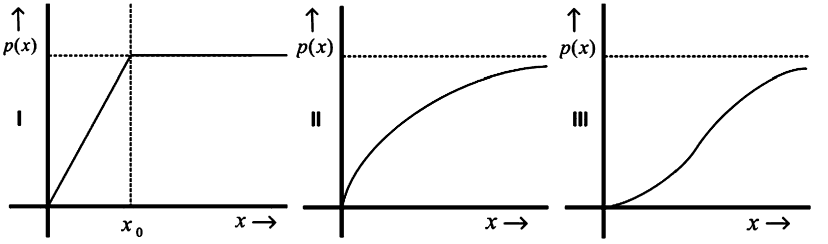

Fig. 1.1. The three types of functional response function, where x represents the prey density, as observed by Holling in experimental data [16].

way to represent biological reality. This leads to so-called phenomenological models to which the Holling models belong. A disadvantage is that the parameters might not always have an intuitive meaning in terms of the original predator-prey ecological system.

On the other hand one could try to derive the functional response function from first principle by demanding that the function satisfies strict fundamental properties of a predator-prey biological system, the so-called mechanistic models. In [20] for example the authors take (among other biological properties like detection and encounter probabilities) the digesting, searching, eating and attacking habits by the predator into account for deriving a suitable functional response. In this approach the parameters should have a more intuitive meaning in terms of the ecological system it is describing, but typically the number of parameters will be larger than in the phenomenological approach. This complicates the mathematical model because each parameter might have a different impact on the result and some parameters might not play a relevant role in the mathematical dynamics.

1.3. Functional response with a cut-off

This paper studies a particular choice for the functional response function in the class of phenomenological models. In the original Holling paper [16] it seems that the observed response function in nature consists of two qualitatively different parts: one strictly increasing function when increasing the prey density below a threshold value and one much flatter function when the prey function exceeds a certain threshold. Holling models this behaviour by three types, of which the last two are differentiable functions. In this paper we consider the first case where the function consists of two parts, i.e. it is piecewise continuous as a function of the underlying prey density. In general one could argue that for modelling predator-prey interaction it could be (especially in phenomenological models) of interest to distinguish between the predator-prey interaction for small and large prey densities, because in some situations it might be difficult to properly model the interaction for large prey densities. See for example [25] where different types of these piecewise functional response functions are studied. In Fig. 1.1 we indicate the basic 3 types which Holling observed from experimental data.

In [36] and [37] the interpretation of introducing a cut-off in the response function is motivated. According to [37] it is plausible that individual predators stop increasing their feeding rates when the prey density exceeds a threshold value: predators will find it easy (since the prey density has exceeded a threshold value) to capture and assimilate prey, but will return to other activities once their ingestion rates are large enough to satisfy their needs.

Other papers using a Holling type I functional response are [3], [4], [27], [30], [32], [36], [37], [40].

In [29] it was shown that the Holling I model can contain two nested limit cycles. It is surprising because the system does not exhibit Hopf-bifurcations and a priori one would expect no limit cycles in such a system.

The purpose of this paper is to investigate the mathematical consequences of choosing a cut-off in the response function. The main results in the next sections will be about the global behaviour of the solutions of the model, in particular the occurrence of limit cycles. For the Holling I model we will prove the existence of two nested limit cycles for a certain range of parameters in the system extending the results of [29]. Furthermore we will show that this is a rigorous upper bound for a particular singular perturbation problem in the Holling I system.

1.4. Functional response of Holling type I

This paper studies the first type of functional response function introduced by Holling. It is possibly the most simple function trying to fit experimental data for predator-prey interaction satisfying some basic properties. Its functional form consists of a linear function combined with a constant function: $p(x) = x$ for $0 \leq x \leq 1$, $p(x) = 1$ for $x > 1$.

On the interval $0 \leq x \leq 1$, representing predator-prey interaction for lower prey densities, the response function is monotonically increasing, a fundamental requirement in these types of models. The fit with experimental data as indicated in [16] is not the most accurate one and can be improved by introducing some nonlinear function. This is outside the scope of this paper (but see for example [25]), where we aim to investigate the effect of introducing a cut-off in the response function for larger prey densities. The Holling type I function is the most elementary type for doing so.

In order to simplify the mathematical formulas we first applied a rescaling in the x-variable to bring the cut-off point between the linear function and the constant function to $x = 1$ (in the original Holling type I the cut-off is a parameter of the system, i.e. x_0). Furthermore we will assume that after an appropriate rescaling of the variables y and t, the conversion rate parameter γ in the Gause model has been scaled to 1.

Summarizing we get the following system of differential equations for the Holling type I predator-prey system:

$$
\begin{aligned}
\frac{dx(t)}{dt} &= \phi x(1 - \frac{x}{k}) - p(x)y, \\
\frac{dy(t)}{dt} &= -\delta y + p(x)y, \\
0 < \delta < 1,\ &\phi > 0,\ k > 2,
\end{aligned}
\tag{1.2}
$$

where $p(x) = x$ for $0 \leq x \leq 1$, $p(x) = 1$ for $x > 1$.
In essence the Holling I system consists of two piecewise quadratic systems.

The variables x and y represent prey and predator densities respectively and are therefore assumed to be non-negative, i.e. we consider system (1.2), in the first quadrant of the phase plane including the line segments $x = 0$, $y \geq 0$ and $y = 0$, $x \geq 0$.

The condition $0 < \delta < 1$ ensures that there exists a singularity in the first quadrant of the phase plane, i.e. an equilibrium with prey and predator densities not equal to zero. For $\delta \geq 1$ no singularities exist in the first quadrant, except for the boundaries. In that case the asymptotic behaviour of the solutions is trivial and we will not consider it here.

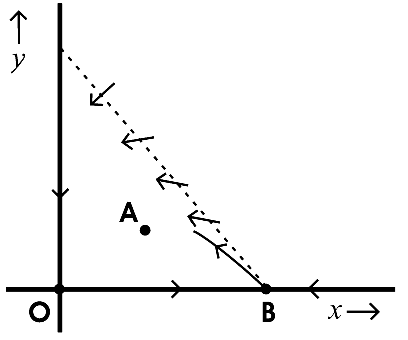

Fig. 2.1. The line without of contact in system (1.2) showing that it is a bounded system (Lemma 2.5).

The parameter k in principle satisfies a more general condition $k > 0$. In the section about Liénard systems we will prove that for $0 < k \leq 2$ no limit cycles occur in system (1.2) and that all solutions will tend to the unique equilibrium point (globally asympotically stable) in the first quadrant outside the axes. Therefore we restrict our investigation to $k > 2$. For $k > 2$ the main problem is to study the appearance of limit cycles in the first quadrant.

2. Local and global properties of the Holling I system

System (1.2) has three real parameters (ϕ, k, δ). We are interested in the qualitative properties of the solutions as a function of these parameters. At the end of the section we will see that this essentially means studying the bifurcation diagram of limit cycles surrounding one singularity in the first quadrant of the phase plane.

Some properties of this system are easy to deduce, so we omit the elementary proofs:

Lemma 2.1. *System (1.2) has a singularity A in the first quadrant, i.e. with $x > 0$, $y > 0$. Its coordinates are ($x = x_g \equiv \delta$, $y = y_g \equiv \phi(1 - \frac{x_g}{k})$). It is a stable anti-saddle. Note that A lies in the strip $0 \leq x \leq 1$.*

Lemma 2.2. *Singularity A in system (1.2) is a node for $\phi \geq \frac{1}{\delta}4(k-\delta)k$ and a focus for $0 < \phi < \frac{1}{\delta}4(k-\delta)k$. In particular the singularity becomes a node for sufficiently large ϕ.*

Lemma 2.3. *System (1.2) has a singularity B on the invariant line $y = 0$. Its coordinates are ($x = k$, $y = 0$). It is a saddle with one unstable separatrix entering the first quadrant. The stable separatrices lie along the invariant line $y = 0$. Note that B lies in the region $x > 1$.*

Lemma 2.4. *System (1.2) has a singularity O at the origin of the phase plane, i.e. with coordinates ($x = 0$, $y = 0$). The stable separatrices lie along the invariant line $x = 0$ of system (1.2). The unstable separatrices lie along the invariant line $y = 0$. Note that O lies in the strip $0 \leq x \leq 1$.*

Lemma 2.5. *System (1.2) is a bounded system. The line tangent to the separatrix of saddle B is a line without contact with all solutions crossing the line inwards (see Fig. 2.1).*

Proof. It is well-known that the tangent line to a separatrix in a quadratic system is a line without contact. This tangent line, which is defined at B in the region $x > 1$, is also a line without contact in the region $0 \leq x \leq 1$.
Define the line l by $y - y_l(x) = 0$, where $y_l(x) \equiv (-\phi - 1 + \delta)(x - k)$. Then we get for $x > 1$:

$$\frac{d}{dt}(y - y_l(x)) = \frac{dy(t)}{dt} - (-\phi - 1 + \delta)\frac{dx(t)}{dt} = \frac{1}{k}(-\phi - 1 + \delta)(x - k)^2\phi < 0,$$

and for $0 \leq x \leq 1$:

$$\frac{d}{dt}(y - y_l(x)) = \frac{dy(t)}{dt} - (-\phi - 1 + \delta)\frac{dx(t)}{dt} = \frac{1}{k}(-\phi - 1 + \delta)(x - k)(\phi x(1 - k) + \delta k(x - 1)) < 0. \quad \square$$

Note 2.6. It is not difficult to check that there are no singularities at infinity (except in the directions $x = 0$ and $y = 0$, but those do not have attracting sectors) in the first quadrant defined by $x > 0,\ y > 0$. The lemma implies that all solutions in the first quadrant are bounded and eventually will enter the triangular region defined by $x > 0$, $y > 0$, $y < (-\phi - 1 + \delta)(x - k)$.

The previous lemmas imply that all solutions starting on or outside the triangular region $x > 0$, $y > 0$, $y < (-\phi - 1 + \delta)(x - k)$ will enter it eventually. Inside this triangular region there is exactly one singularity which is stable. According to the Poincaré-Bendixson theorem this implies that all solutions will either approach the singularity A or a limit cycle surrounding A when $t \to \infty$. Due to the stability of the singularity A in Lemma 2.1 we can conclude:

Proposition 2.7. *System* (1.2) *has an even number of nested limit cycles surrounding the singularity A, counting multiplicity.*

We will see in the following that situations with no limit cycles, one semistable limit cycle or two hyperbolic limit cycles can each occur for this system.

Finally we point out some results about non-existence of limit cycles in (1.2). In order to do so we introduce the so-called Liénard form of the system. For the study of limit cycles it is well-known that some of the strongest global results have been obtained for systems in a so-called Liénard form, especially by researchers in China and Russia. See for example [39] where powerful theorems are presented.

The generalized Liénard system has the following structure:

Definition 2.8. Generalized Liénard system:

$$\begin{aligned} \frac{dx(t)}{dt} &= F(x) - \psi(y), \\ \frac{dy(t)}{dt} &= g(x), \end{aligned} \tag{2.1}$$

defined on some open strip $x \in (x_-, x_+)$, $y \in (y_-, y_+)$.

There are different ways to transform the system (1.2) into the form of a generalized Liénard system. We are aware of four different ways but will use only one in the following. The other forms may provide additional information to study the behaviour of limit cycles but we have not been successful in doing so.

The transformation from system (1.2) to this form is not difficult to find, because it only requires a rescaling in the time variable $t \to \frac{t}{p(x)}$ and change of variable $y = e^u$ (and renaming $u \to y$):

Lemma 2.9. *System (1.2) can be brought into generalized Liénard form (2.1) with:*

$$\begin{aligned} F(x) &= \phi(1-\frac{x}{k}),\ for\ 0<x\leq 1;\ \ F(x)=\phi x(1-\frac{x}{k}),\ for\ x>1,\\ g(x) &= \frac{x-\delta}{x},\ for\ 0<x\leq 1;\ \ g(x)=1-\delta,\ for\ x>1,\\ \psi(y) &= e^y, \end{aligned} \tag{2.2}$$

with $x \in (x_-, x_+) = (0, \infty)$, $y \in (y_-, y_+) = (-\infty, \infty)$.

Lemma 2.10. *The divergence of system (2.2) is given by* $f(x) = \frac{dF(x)}{dx}$*:*

$$f(x) = -\frac{\phi}{k},\ for\ 0<x\leq 1;\ \ f(x)=\phi(1-\frac{2x}{k}),\ for\ x>1. \tag{2.3}$$

To find parameter values for which no limit cycles occur, we need a slight modification of an application of Green's theorem. Since we are dealing here with a system that has a discontinuity at $x = 1$ for the divergence $f(x)$, we need to make an adjustment. A well-known theorem is that for the generalized Liénard system (2.1) the area-integral of $f(x) \equiv \frac{dF(x)}{dx}$ over the interior of a periodic solution Γ is equal to 0, when $f(x)$ is continuous for all x. This can be extended to the case where it is only piecewise continuous. For a proof, see Appendix A.

Lemma 2.11. *For any periodic orbit* Γ *with* $x = x_\gamma(t)$, $y = y_\gamma(t)$, *periodic functions satisfying* (2.1), *where* $F(x)$ *is continuous and* $f(x) \equiv F'(x)$ *is continuous except at isolated points (where it makes a finite jump), the following relationship is true:*

$$\iint_{int(\Gamma)} f(x)dxdy = 0. \tag{2.4}$$

In our case the system is piecewise differentiable and Lemma 2.11 can be used in the next proofs.

Notice that $f(\delta) < 0$, confirming that the singularity in the first quadrant is stable. Moreover $f(x) < 0$, for $0 \leq x \leq 1$, which implies that:

Lemma 2.12. *Limit cycles of system (1.2) need to cross the line* $x = 1$.

Proof. A limit cycle of system (1.2), if it exists, will surround the singularity A lying in the region $0 \leq x \leq 1$. Therefore part of any limit cycle necessarily lies in $0 \leq x \leq 1$. Since the area-integral of the divergence over the interior of any period solution is equal to zero (Lemma 2.11), and since $f(x) < 0$ for $0 \leq x \leq 1$, part of the limit cycle needs to lie in the region $x > 1$ as well. □

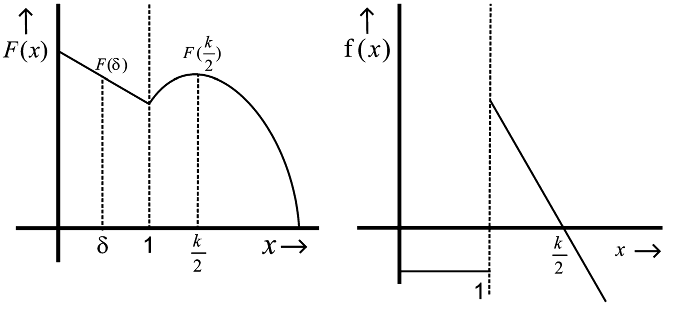

Fig. 2.2. The functions $F(x)$ in (2.2) and divergence $f(x)$ in (2.3) for $k > 2$.

A necessary condition on the parameters for the existence of limit cycles can be given using a theorem from the theory of Liénard systems. It involves checking the function $F(x)$ in (2.1). The function $F(x)$ in (2.2) is a decreasing straight line on the interval $0 \leq x \leq 1$. If $k > 2$, then it is continuous across $x = 1$ and continues as a downward parabola with a maximum at $x = \frac{k}{2}$ for $x > 1$. If $k \leq 2$, then $f(x)$ is negative for all $x > 0$: no limit cycles occur, because the divergence of the vector field is negative in the first quadrant of the phase plane. See Fig. 2.2 for the situation when $k > 2$. Therefore we can conclude that:

Lemma 2.13. *A necessary condition for the existence of limit cycles in system* (1.2) *is* $k > 2$.

Under the condition $k > 2$, the function $F(x)$ has a maximum for $x = \frac{k}{2} > 1$. Next we can deduce another non-existence condition by investigating under which condition the system:

$$F(x_1) = F(x_2), \tag{2.5}$$

does not have a non-trivial solution pair $0 < x_1 < \delta < x_2$. The equation $F(x_1) = F(x_2)$ can only have non-trivial solutions (i.e. define a real curve $x_1 = \tau(x_2)$), such that $F(\tau(x_2)) = F(x_2)$) if the maximum of the function $F(x)$ at $x = \frac{k}{2}$ lies above $F(\delta)$. Otherwise all points of the graph $y = F(x)$ for $x > \delta$ will lie below the points of $y = F(x)$ for $x < \delta$ and the equation (2.5) cannot have solutions.

The condition that there are no solutions to (2.5) translates into:

$$F(\delta) > F(\frac{k}{2}).$$

This leads to the inequality:

$$\phi(1 - \frac{\delta}{k}) > \frac{\phi k}{2}(1 - \frac{\frac{k}{2}}{k}) = \frac{\phi k}{4},$$

which can be rewritten in the form:

$$k^2 - 4k + 4\delta < 0. \tag{2.6}$$

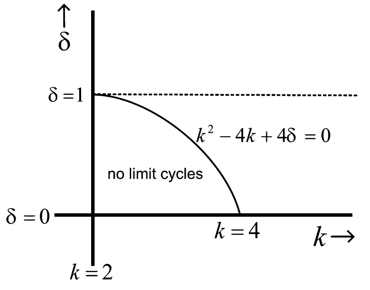

Fig. 2.3. Regions in the (k, δ) parameter space with fixed ϕ for which system (1.2) does not have limit cycles.

If this condition is satisfied, then no limit cycles can occur in the Holling I system as we will show. In order to achieve this we state the following powerful theorem for Liénard systems for the non-existence of limit cycles:

Theorem 2.14. *[39] If the functions in* (2.1) *satisfy the following conditions:*

1. $(x - x_g)g(x) > 0$ *for* $x \neq x_g$,
2. $\frac{d\psi(y)}{dy} > 0$,
3. *The system of equations:*

$$F(x_1) = F(x_2),$$
$$G(x_1) = G(x_2),$$

where $G(x) \equiv \int_{x_g}^{x} g(\bar{x})d\bar{x}$ *has no solutions* $x_- < x_1 < x_g$, $x_g < x_2 < x_+$,

then no limit cycle surrounds the singularity at $(x = x_g, y = y_g)$.

Since we have identified a parameter set for which the equation $F(x_1) = F(x_2)$ does not have non-trivial solutions, we can immediately apply Theorem 2.14 and conclude from the parameter condition (2.6):

Lemma 2.15. *No limit cycles exist for system* (1.2) *if* $k^2 - 4k + 4\delta < 0$.

Notice that the parameter set $k^2 - 4k + 4\delta = 0$ passes through the two points $(k = 2, \delta = 1)$ and $(k = 4, \delta = 0)$ in the (k, δ)-parameter plane. See Fig. 2.3.

3. The Holling I system with $\delta = 1 - \epsilon$, $0 < \epsilon \ll 1$

For $\delta = 1$ system (1.2) partially degenerates, see also [29].

In the region $0 \leq x \leq 1$ system (1.2) remains regular, but singularity A has moved to the boundary line at $x_g = 1$ with $y_g = \phi(1 - \frac{1}{k})$.

In the part of the phase plane where $0 \leq x \leq 1$ we do not know the solution curves explicitly, only their qualitative behaviour.

In the region $x > 1$ the system (1.2) degenerates: the phase plane consists of horizontal lines $y = c$, where $c > 0$, and a continuum of singularities lying on the parabola $y = \phi x(1 - \frac{x}{k})$. This

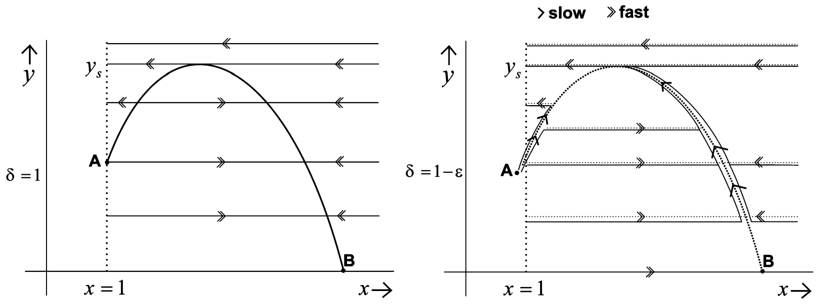

Fig. 3.1. The degenerate system (1.2) with $\delta = 1$ and $\delta = 1 - \epsilon$ in the region $x > 1$, where we indicated that for small ϵ the singularity A has moved into the region $x < 1$.

continuum is attached on its left boundary, i.e. at $x = 1$, to the limiting position of the singularity A. We consider in this paper the case where A is a focus following [29]. In [29] the focus case was considered without explicitly stating this. According to Lemma 2.2 for fixed parameters δ, k, the singularity becomes a node when ϕ is taken large enough. This node-case is much more complex to handle. In a future paper we will consider this bifurcation mechanism.

3.1. The phase portrait of the system for $\delta = 1$ and $\delta = 1 - \epsilon$

3.1.1. The region $x > 1$

System (1.2) degenerates for $\delta = 1$, $x > 1$. The phase portrait consists of horizontal lines $y = c$, $c > 0$ and a continuum of singularities lying on the parabola $y = \phi x(1 - \frac{x}{k})$. Below (above) the parabola the solutions on the horizontal line $y = c$ move to the right (left) with increasing time (Fig. 3.1). After perturbation, i.e. $\delta = 1 - \epsilon$, $0 < \epsilon \ll 1$, the system becomes regular and the unstable separatrix leaving the saddle B at $(x = k, y = 0)$ emerges from the continuum of singularities for $x \in (\frac{k}{2}, k)$ and from the horizontal solution $y = \frac{\phi k}{4}$ for $x \in (1, \frac{k}{2})$. The separatrix enters the system defined for $0 \le x \le 1$ of system (1.2), approximately at the point $(x = 1, y = y_s \equiv \frac{\phi k}{4})$.

In system (1.2) with $\delta = 1$ all fast solutions either reach $x = 1$, with $y > y_g$, or they reach the parabola $y = \phi x(1 - \frac{x}{k})$ for $\frac{k}{2} < x < k$. In particular of interest is that the solutions starting at $(x = 1, y = y_1 < y_g)$ will approach the parabola for $\frac{k}{2} < x < k$. After perturbation, i.e. $\delta = 1 - \epsilon$, the parabola $y = \phi x(1 - \frac{x}{k})$ becomes a curve without contact in $x > 1$, because $\frac{dx}{dt} = 0$ and $\frac{dy}{dt} > 0$. It follows that the fast solutions starting at $(x = 1, y = y_1 < y_g)$ after perturbation will reach the parabola along an approximate horizontal line near $(x = x_2, y = y_1)$, where $\frac{k}{2} < x_2 < k$ satisfies $y_1 = \phi x_2(1 - \frac{x_2}{k})$. Due to the direction of the vector field of the perturbed system (i.e. $\frac{dy}{dt} > 0$ for $x > 1$) the solution then continues along the parabola (the "slow"-part) until it reaches the peak near $(x = \frac{k}{2}, y = \frac{\phi k}{4})$. At the peak it is easy to see that all solutions reaching it will continue along the fast solution following the approximate horizontal line $y = y_s = \frac{\phi k}{4}$ reaching a point on $x = 1$ near $y = y_s$.

This can be seen by checking the vector field of the perturbed system, but can also be formally deduced from the fact that the peak is a so-called canard point (see [5]). See Fig. 3.1.

In conclusion we find:

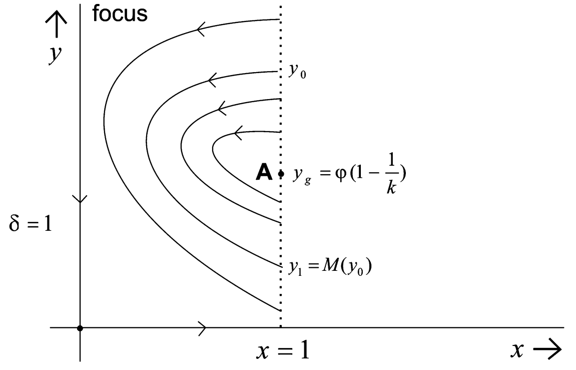

Fig. 3.2. The system (1.2) with $\delta = 1$ in the region $0 \le x \le 1$ when the singularity A is a focus.

Lemma 3.1. *For system (1.2) in the region $x > 1$, after perturbation $\delta = 1 - \epsilon$ solutions starting at the boundary $(x = 1, y = y_0 < y_g)$ will reach a point near $(x = 1, y = y_s)$.*

3.1.2. The region $0 \le x \le 1$

The system defined in the left strip $0 \le x \le 1$, i.e. (1.2) is regular for $\delta = 1$. For $0 < \phi < 4k(k-1)$ the phase plane is filled with the solution curves of a system with a singularity of focus type which has collapsed onto the boundary line $x = 1$ at the point with y-coordinate $y_g \equiv \phi(1 - \frac{1}{k})$. To describe the properties of the solutions, consider a starting point $(x = 1, y_0 > y_g)$ on the vertical boundary line. In the case of a focus the solution starting at such a point will reach the boundary line $x = 1$ in finite time again with a y-coordinate which we denote by $y_1 = M(y_0)$, where $y_1 < y_g$, i.e. below the collapsed singularity. Moreover we have $\frac{dM(y_0)}{dy_0} < 0$. See Fig. 3.2.

3.2. Slow-fast cycles for $\delta = 1 - \epsilon$, $0 < \epsilon \ll 1$

Next we combine the results of the previous two sections to make a statement about solutions forming a closed (i.e. periodic) solution after perturbation $\delta = 1 - \epsilon$.

3.2.1. Singular cycles passing below the singularity A

First we consider the situation when periodic solutions are created in the slow-fast system from a cycle passing through a point $(x = 1, y = y_0 < y_g)$. These can only occur from the limiting position formed by the fast solution in the region $0 \le x \le 1$ which starts at $(x = 1, y = y_s)$ and which reaches some point $(x = 1, y = \bar{y}_1 < y_g)$. Any other fast solution reaching $(x = 1, y = y_0 < y_g)$, i.e. not starting at $(x = 1, y = y_s)$ will return in the region $x > 1$ always to the point near $(x = 1, y = y_s)$ and does not form a closed cycle. See Fig. 3.3.

Lemma 3.2. *Consider a periodic solution of (1.2) with $\delta = 1 - \epsilon$, created from a singular cycle in system (1.2) with $\delta = 1$ passing through a point $(x = 1, y = \bar{y}_1 < y_g)$. Then the singular cycle necessarily will through the point $(x = 1, y = y_s)$. The point $(x = 1, y = \bar{y}_1)$ lies on the solution curve in $0 \le x \le 1$ of (1.2) with $\delta = 1$, passing through $(x = 1, y = y_s)$.*

The discussion above covers the possible limit cycle perturbations from the slow-fast system (1.2) with $\delta = 1$, but did not address the case of the creation of small-amplitude limit cycles from a single singularity in the continuum of singularities when $\delta = 1$. Since limit cycles after

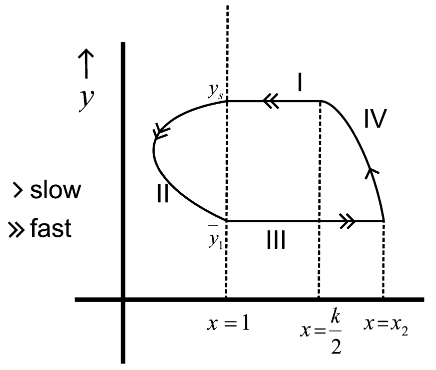

Fig. 3.3. The singular cycle from which a periodic solution may be perturbed in the system (1.2) with $\delta = 1$, passing through a point $(x = 1, y = \bar{y}_1 < y_g)$, case Γ_{big} in Proposition 3.3.

perturbation need to cross the vertical line $x = 1$, no singularity in the region $x > 1$ can produce such a small-amplitude limit cycle. The only singularity which possibly can produce a small-amplitude limit cycle is the degenerate end point $(x = 1, y = y_g)$ at the boundary $x = 1$. We will see in the next section that in the case of a focus, such a small-amplitude limit cycle will indeed be created after perturbation.
Summarizing we get the following two types of bifurcation mechanisms for the slow-fast system for $\delta = 1$. Note that the proposition does not not make a statement about the existence of such limit cycles. It merely indicates the possible limiting positions which need to be investigated.

Proposition 3.3. *Limit cycles may be created after perturbation from a cycle Γ in the singular system (1.2) with $\delta = 1$ according to two possible mechanisms:*

1. *Small-amplitude cycle Γ_{small}: from the singularity A at $(x = 1, y = y_g = \phi(1 - \frac{1}{k}))$.*
2. *Duck cycle without a head Γ_{big}: a slow-fast cycle, consisting of the union of solution curves*
   - I) *a fast solution $y = y_s \equiv \frac{\phi k}{4}$ for $x \in (1, \frac{k}{2})$,*
   - II) *a fast solution starting at $(x = 1, y = y_s)$ in the region $0 \le x \le 1$ satisfying the regular system (1.2) with $\delta = 1$ until it reaches a point $(x = 1, y = \bar{y}_1 < y_g)$,*
   - III) *a fast solution $y = \bar{y}_1$ for $x \in (1, x_2)$ such that $y = \bar{y}_1 \equiv \phi x_2(1 - \frac{x_2}{k})$, i.e. until it reaches the continuum of singularities lying on a parabola,*
   - IV) *a slow section lying on the parabola $y = \phi x(1 - \frac{x}{k})$ for $x \in (\frac{k}{2}, x_2)$.*

In Fig. 3.3 the situation of Γ_{big} depicted.

3.3. Stability of the limit cycle perturbed from the slow-fast cycle Γ_{big}

In the generalized Liénard system (2.1) the characteristic exponent of a period solution Γ is given by $\oint_\Gamma f(x)dt$, where $f(x) \equiv \frac{dF(x)}{dx}$ is continuous for all x corresponding to the periodic solution. We generalize this result to the situation where $f(x)$ has a finite number of discontinuity points. The proof is given in Appendix B. For piecewise linear systems a similar result was already proved in [14].

Lemma 3.4. *For any periodic orbit* Γ *with* $x = x_\gamma(t),\ y = y_\gamma(t)$, *periodic functions satisfying* (2.1), *where* $F(x)$ *is continuous and* $f(x) \equiv F'(x)$ *is continuous except at isolated points where it makes a finite jump, the characteristic exponent of the periodic orbit is given by:*

$$\oint_\Gamma f(x)dt. \tag{3.1}$$

The characteristic exponent of the period solution determines its stability. In particular if it is < 0 (> 0), then it is a hyperbolic stable (unstable) limit cycle. If it is equal to 0, then the periodic solution is not hyperbolic and its stability depends on higher order integrals.

Note that in the case of the Liénard system corresponding to the Holling type I system (1.2), i.e. system (2.2), the function $f(x)$ is differentiable for all $x \geq 0$ except for $x = 1$. The above lemma holds true because there is only one discontinuity point.

An extensive literature exists for the study of limit cycles created after perturbation from systems with a continuum of singularities (see [5], [6], [7], [8], [9], [10], [11], [26]). In this paper we do not need the full scope of their theorems. For the global bifurcation of limit cycles from a singular system, the stability of the limit cycle is determined by the integral of the divergence $f(x)$ along the cycle according to Lemma (3.4). In the case of slow-fast systems this integral is dominated by the integral of the divergence of the perturbed system along the slow parts of the unperturbed system. In the case of Holling I this gives an easy way to estimate an upper bound on the number of limit cycles.

By studying the integral of the perturbed divergence along the slow parts of the singular cycles, we can estimate the stability of the perturbed limit cycles. The justification for doing this can be found in [11]. The most convenient form to achieve this, is the Liénard form of the system. Since the slow parts of the cycle all lie in the region $x > 1$, we can restrict our calculation to that region. The only exception is the small-amplitude limit cycle Γ_{small} in Proposition 3.3 which is created from a singularity lying on the boundary line $x = 1$. That case is covered in the next section.

The Liénard form of (1.2) with $x > 1$ is:

$$\begin{aligned}
&\frac{dx(t)}{dt} = F(x) - \psi(y),\\
&\frac{dy(t)}{dt} = g(x),\\
&F(x) = \phi x(1 - \frac{x}{k}),\\
&g(x) = 1 - \delta,\\
&\psi(y) = e^y,\\
&x > 1,\ y \in \mathbb{R}.
\end{aligned} \tag{3.2}$$

In particular the divergence of this system is given by:

$$f(x) \equiv \frac{dF(x)}{dx} = \phi(1 - \frac{2x}{k}). \tag{3.3}$$

The stability of the perturbed cycle will be determined by the sign of the following integral:

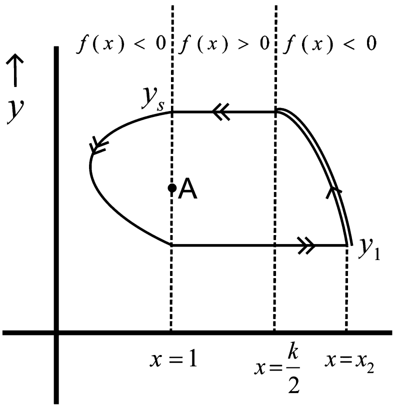

Fig. 3.4. Sign of the divergence of (3.3) for case Γ_{big} in Proposition 3.3.

$$\oint_{slow\ sections} f(x)dt = \oint_{slow\ sections} \phi(1 - \frac{2x}{k})dt. \tag{3.4}$$

This can be deduced in a formal way by making estimates on the full contour integral along the cycle, but intuitively it is clear that the slow part will determine the sign of the integral because $f(x)$ is bounded and dt is finite along the fast parts of the cycle, while it will approach infinity along the slow parts.

The divergence (3.4) is negative (positive) for $x > \frac{k}{2}$ $(1 < x < \frac{k}{2})$ which implies immediately the stability of the perturbed cycle in Proposition 3.3:

Proposition 3.5. *A limit cycle perturbed from cycle Γ_{big} in Proposition 3.3 is hyperbolic and stable.*

Proof. The slow part cycle Γ_{big} lies in the strip $\frac{k}{2} < x < k$, where according to (3.3) the divergence is negative. It follows that the sign of the characteristic exponent (3.4) is negative. The limit cycle, if it exists, is therefore hyperbolic and stable. See Fig. 3.4. □

A direct consequence is that at most one limit cycle can be created from the cycle Γ_{big}. It is impossible for two adjacent nested limit cycles to be both unstable so we can immediately conclude that only one limit cycle is created in this mechanism:

Proposition 3.6. *At most one limit cycle can be created from the headless duck cycle Γ_{big} after perturbation of the singular system (1.2) with $\delta = 1$. It is hyperbolic and stable, if it exists.*

4. Bifurcation of a small-amplitude limit cycle Γ_{small} for $\delta = 1 - \epsilon$

In this section we study the bifurcation of a small-amplitude limit cycle from the singular system (1.2) with $\delta = 1$ as indicated in Proposition 3.3, case Γ_{small}: the cycle created from the singularity A at $(x = 1, y = y_g = \phi(1 - \frac{1}{k}))$. It also provides a natural way to prove that two limit cycles are created from the singular system.

4.1. Blow-up of the singularity

In order to study the behaviour of the system near the boundary point of the continuum of singularities, we apply a blow-up transformation to the original Holling I system (1.2). First we move the singularity A with coordinates $(x = x_g = \delta, y = y_g = \phi(1 - \frac{\delta}{k}))$ to the origin through the translation $x = \bar{x} + \delta$, $y = \bar{y} + \phi(1 - \frac{\delta}{k})$, after which we apply the blow-up $\bar{x} = (1 - \delta)\tilde{x}$, $\bar{y} = (1 - \delta)\tilde{y}$. We scale the time variable by $t \to kt$ and obtain (after dropping the tilde on the variables for notational convenience):

$$\begin{aligned}
\frac{dx(t)}{dt} =& P_0(x, y) + \epsilon P_1(x, y),\\
\frac{dy(t)}{dt} =& Q_0(x, y) + \epsilon Q_1(x, y),\\
P_0(x, y) =& -\phi x - ky,\ \frac{\epsilon - 1}{\epsilon} for \le x \le 1;\ P_0(x, y) = \phi(k-2)x - ky - \phi k + \phi,\ for\ x > 1,\\
P_1(x, y) =& (1 - x)(\phi x + ky),\ \frac{\epsilon - 1}{\epsilon} for \le x \le 1;\ P_1(x, y) = -\phi(x-1)^2,\ for\ x > 1,\\
Q_0(x, y) =& \phi(k-1)x,\ \frac{\epsilon - 1}{\epsilon} for \le x \le 1;\ Q_0(x, y) = \phi(k-1),\ for\ x > 1,\\
Q_1(x, y) =& (\phi + ky)x,\ \frac{\epsilon - 1}{\epsilon} for \le x \le 1;\ Q_1(x, y) = (\phi + ky),\ for\ x > 1.
\end{aligned} \tag{4.1}$$

The above system is topologically equivalent to the original system and contains the same number of limit cycles. The main difference is that for small ϵ, i.e. the perturbation of limit cycles from the singular system when $\delta = 1$, in system (4.1) the globally perturbed limit cycle from the slow-fast system (i.e. Γ_{big} mentioned in Proposition 3.3) appears at infinity while the small-amplitude limit cycles created from the end-point of the continuum of singularities in the original system (i.e. singularity A) have been blown up and have become regular-sized periodic solutions. So in order to study the creation of small-amplitude limit cycles of the original system with δ near 1, we need to investigate how many limit cycles can be created from the finite part of the phase plane in system (4.1).

4.2. The unperturbed blown-up system

We observe that for $\epsilon = 0$, the system (4.1) is defined by two piecewise linear systems:
For $-\infty \le x \le 1$

$$\frac{dx(t)}{dt} = -\phi x - ky,\quad \frac{dy(t)}{dt} = \phi(k-1)x. \tag{4.2}$$

For $x > 1$:

$$\frac{dx(t)}{dt} = \phi(k-2)x - ky - \phi k + \phi,\quad \frac{dy(t)}{dt} = \phi(k-1). \tag{4.3}$$

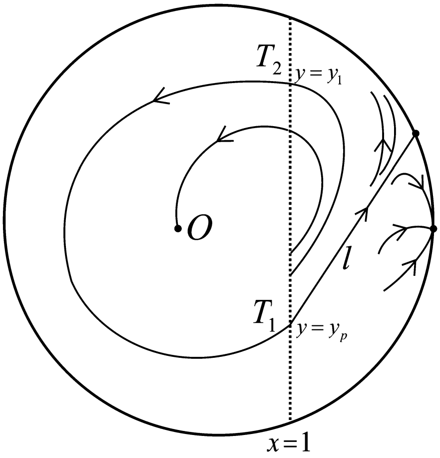

Fig. 4.1. Invariant line and phase portrait of the system (4.3) with $\epsilon = 0$ for the focus case, depicted on the Poincaré sphere.

For system (4.2) and (4.3) we want to prove that after bifurcation at most one (unstable) limit cycle appears created from the finite part of the plane.

The unperturbed system has one singularity at the origin defined by the first system (4.2). As expected it is a regular stable focus for $0 < \phi < 4(k-1)k$, the case which we are considering here.

The important property of this system is the existence of an invariant line for $x > 1$:

Lemma 4.1. *If* $0 < \phi < 4(k-1)k$, *then system* (4.2) *has a focus and does not have invariant lines.*
System (4.3) *has one invariant line* l *given by* $y = y_l(x) \equiv \frac{\phi(k-2)}{k}x - \frac{(k-1)(k+(k-2)\phi)}{k(k-2)}$. *System* (4.3) *has two singularities at infinity: a saddle with a stable separatrix entering it from the finite part of the phase plane, formed by the invariant line* l, *and a stable node at the end of the* x*-axis. See Fig. 4.1 where the phase portrait is shown on the Poincaré sphere.*

Proof. The first statement follows from an elementary calculation by looking for invariant solutions of the form $y = \lambda_1 x + \lambda_0$. The other statements can be most easily deduced by investigating the first integral of the system:

$$x = \frac{k}{\phi(k-2)}y + \frac{k-1}{k-2} + \frac{k(k-1)}{\phi(k-2)^2} + C_1 e^{\frac{k-2}{k-1}y}.$$

For $C_1 = 0$ we retrieve the invariant line and for $C_1 > 0$ the solutions approach the stable node at the end of the x-axis, while for $C_1 < 0$ the solutions lie above the invariant line l and return to the line $x = 1$ as depicted in Fig. 4.1. $\square$

The first result of the lemma is natural because the linear system (4.2) will have no invariant lines in the case of a focus. The second result is important because it shows the existence of a solution starting at $x = 1$ moving to infinity and will imply the existence of an unstable limit cycle as shown in the next proposition. The interpretation of the two singularities at infinity is

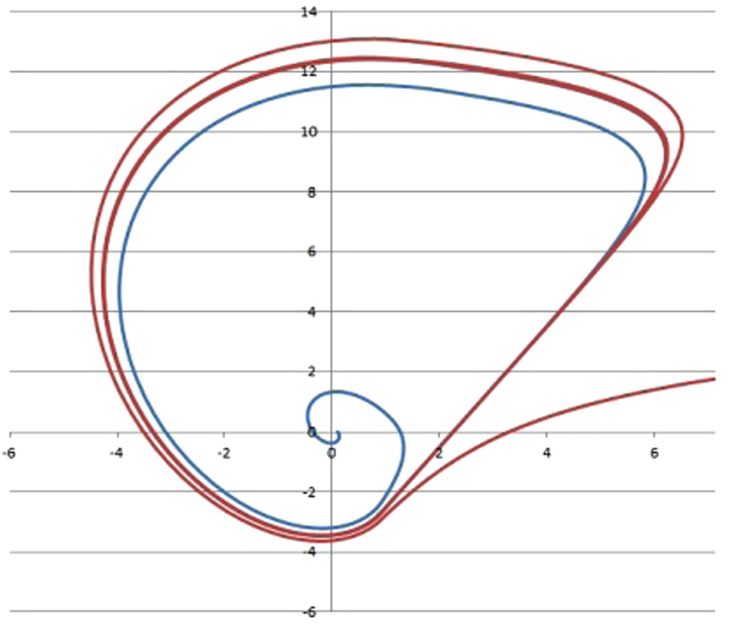

Fig. 4.2. Numerical picture of a limit cycle occurring in the unperturbed blown-up system (4.2), (4.3).

that the invariant line l forms the stable separatrix continuing in the original system (1.2) before blow-up in the channel formed by slow solutions along $y = \phi x(1 - \frac{x}{k})$, while the solutions approaching the stable node at infinity will continue in the original system along the channel formed by fast solutions along $y = y_g$. The blow-up shows that no solutions enter the system from infinity showing that the blown-up system provides an ϵ-neighborhood of the singularity at $x = 1$, $y = y_g$ containing an unstable limit cycle:

Proposition 4.2. *If the origin is a focus, i.e. $0 < \phi < 4(k-1)k$, exactly one hyperbolic unstable limit cycle exists in the phase plane of system* (4.2)*,* (4.3)*. Exactly one unstable hyperbolic limit cycle will be created from the finite part of the phase plane under the perturbation of δ in the blown up system* (4.1)*, i.e. a hyperbolic unstable small-amplitude limit cycle of the type Γ_{small} in Proposition 3.3 will occur.*

Proof. The first part of the proof concerns the existence of the limit cycle. Consider the invariant line solution l in the region $x > 1$ as described in Lemma 4.1. When t increases, the solution along the invariant line will tend to infinity. The line is connected to the boundary line $x = 1$ at the point T_1, $(x = 1, y = y_p \equiv y_l(1))$. In the region $-\infty < x \leq 1$ this solution continues as part of the phase plane of a linear focus. It will reach $x = 1$ again at a point T_2 with coordinates $(x = 1, y = y_1 > y_p)$. Consider the α-limit set of the solution starting at T_2. It cannot tend to the singularity at the origin because that singularity is stable and it cannot tend to any other (finite or infinite) point in $x > 1$. Since there are no other singularities left, it has to approach a limit cycle which is unstable from the outside. Similary we can see that the limit cycle is unstable on the inside as well, because the α-limit set of the solutions coming to the stable focus can only be the limit cycle surrounding the origin. See Figs. 4.1 and 4.2.

Another way to prove the existence of the unstable limit cycle would be to write down explicitly the Poincaré mapping at the line $x = 1$. This is possible because both linear systems can be integrated explicitly. It leads to the same result but the computation is much more cumbersome.

Next we need to prove that the unstable limit cycle is unique and hyperbolic. First we write the blown-up system in the form of a Liénard system. After a scaling in time $t \to \frac{t}{k}$ the system (4.2), (4.3) takes the form of a Liénard system (2.1) with:
For $-\infty \leq x \leq 1$:

$$\begin{aligned} F(x) &= -\frac{\phi}{k}x, \\ g(x) &= \frac{\phi(k-1)}{k}x, \\ \psi(y) &= y. \end{aligned} \tag{4.4}$$

For $x > 1$:

$$\begin{aligned} F(x) &= \frac{\phi(k-2)}{k}x - \phi + \frac{\phi}{k}, \\ g(x) &= \frac{\phi(k-1)}{k}, \\ \psi(y) &= y. \end{aligned} \tag{4.5}$$

The derived quantity $f(x)$, i.e. the divergence of the system takes the form:
For $-\infty \leq x \leq 1$:

$$f(x) = -\frac{\phi}{k}. \tag{4.6}$$

For $x > 1$:

$$f(x) = \frac{\phi(k-2)}{k}. \tag{4.7}$$

We apply a theorem for Liénard systems which proves the uniqueness and hyperbolicity of a limit cycle under certain conditions. It is a version of the well-known Zhang Zhifen theorem where the hyperbolicity of the limit cycle was proved using a Filippov-transformation (see [39]). The proof relies on the formula of the characteristic exponent along a periodic orbit as described in Lemma 3.4. Since the formula is the same for piecewise differentiable Liénard systems, we can apply the uniqueness theorem to our case as well.

For system (4.4), (4.5) we can check the conditions of the following uniqueness theorem:

Theorem 4.3. *[41] If the functions in* (2.1) *satisfy the following conditions:*

1. $xg(x) > 0$ *for* $x \neq 0$,

2. $(x - x_f) f(x) > 0$, $x \neq x_f$, $x_f > 0$,
3. $\frac{d\psi(y)}{dy} > 0$,
4. $\frac{f(x)}{g(x)}$ *is nondecreasing in* $x < 0$ *and* $x > x_f$,

then the system has at most one limit cycle surrounding the singularity at $x = 0$ *which is hyperbolic if it exists.*

It is easy to see that the first three conditions of the theorem are satisfied by system (4.4), (4.5) with $x_f = 1$. The critical fourth condition becomes in this case:
For $-\infty \leq x \leq 1$

$$\frac{d}{dx}\frac{f(x)}{g(x)} = \frac{1}{(k-1)x^2} > 0.$$

For $x > 1$:

$$\frac{d}{dx}\frac{f(x)}{g(x)} = 0.$$

It follows that all conditions of the uniqueness theorem are satisfied and we finally arrive at Proposition 4.2. Note that the point of discontinuity at $x = 1$ does not take part in the calculation of the quantities in the fourth condition. □

Note 4.4. In [31] the uniqueness and hyperbolicity of the limit cycle were proved for a similar system. However, in that paper they consider the case where the point of discontinuity passes through the singularity at the origin.

Since we know from Proposition 2.7 that an even number of limit cycles occurs in the original Holling I system, we have to conclude that a second limit cycle is created which is stable in the case of a focus. In the case of a focus we only have two mechanisms for creating a limit cycle after perturbation according to Proposition 3.3: a small-amplitude limit cycle from Γ_{small} (which we have just proved to be unique, hyperbolic and unstable) and from Γ_{big} which according to 3.5 is hyperbolic and stable. Therefore we can conclude:

Theorem 4.5. *Exactly two limit cycles are created under the perturbation of* $\delta = 1 - \epsilon$, $0 < \epsilon \ll 1$ *of the singular system* (1.2) *with* $\delta = 1$, *if the singularity is a focus* ($0 < \phi < 4k(k-1)$). *One hyperbolic unstable small-amplitude limit cycle is created from the singularity* A *at* ($x = 1$, $y = \phi(1 - \frac{1}{k})$), Γ_{small} *as described in Proposition 3.3 and one hyperbolic stable limit cycle is created from the singular cycle* Γ_{big} *as described in Proposition 3.3.*

Note 4.6. In [29] the existence of two limit cycles was announced, but the condition that A needs to be a focus was not mentioned.

5. Discussion

The results of this paper suggest that the maximum number of limit cycles of the Holling type I system (1.2) is two. In Fig. 5.1 a numerical picture is shown with a typical situation with two

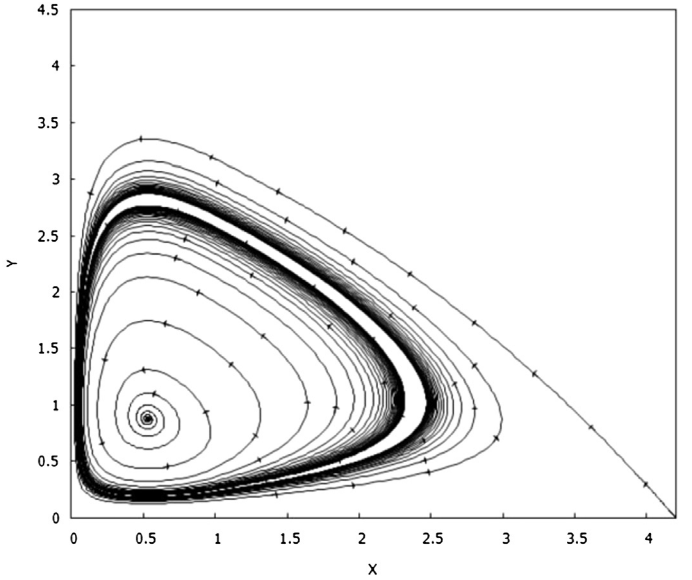

Fig. 5.1. Numerical picture of two limit cycles in the Holling type I system (1.2) for $k = 4.2$, $\delta = 0.52$, $\phi = 1$.

limit cycles for parameter values $k = 4.2$, $\delta = 0.52$, $\phi = 1$. It shows that even for values far from $\delta = 1$ two limit cyles can persist.

The difficulty in the analysis of the system lies in the fact that no weak focus or saddle connections occur and simple bifurcation techniques do not apply. The logical choice for the investigation of the system then is to study the limiting behaviour of the system at the boundary of the parameter ranges. In this paper we considered the boundary $\delta = 1$. The other choices we will discuss in future work, i.e. $\phi = 0$, $\phi = \infty$, $k = \infty$, $\delta = 0$. Our preliminary results show that also in those cases at most two limit cycles will occur after perturbation.

In this paper we discussed the case where the singularity A is a focus. The case where A is a node (not discussed in [29]) leads to much more complex behaviour. In a future paper we will discuss the limit cycle bifurcation for this case when $\delta = 1$. The possible limiting cases are of a different type than in the case of a focus. These include so-called canards with and without a head.

Some of the results of this paper for the Holling type I system can be extended to a more general case of the Gause system (1.1), i.e. more general functions $h_1(x)$ and $p(x)$ (where $p(x)$ has a cut-off, i.e. $p(x)$=1 for $x > 1$) but still with $h_2(y) = \delta y$. For $\delta = 1$ similar singular perturbations will occur as for the ones discussed in this paper and an estimate on the upper bound of perturbed limit cycles can be made in terms of general functions $h_1(x)$ and $p(x)$ in (1.1). This general case will be published in a future paper.

In general the results of this paper show that the introduction of a cut-off value in the function response function $p(x)$ can lead to more complex behaviour than for an analytical functional response function. It implies that when fitting experimental data with a functional form for $p(x)$ it is important to investigate the impact of the behaviour for large x: apparently small differences in the behaviour of the function (compare for example the Holling type I and type II functional response functions) can lead to large differences in the behaviour for small x, i.e. in the finite part of the phase plane.

Acknowledgments

The authors would like to thank Prof. De Maesschalck for pointing out and correcting some mistakes in the original draft. The authors would also like to express their gratitude to the referee whose review improved the paper greatly.

Appendix A. Divergence theorem for piecewise differentiable Liénard systems

This appendix contains the proof of Lemma 2.11.

We consider the generalized Liénard system (2.1) where we write $\frac{dx}{dt} \equiv P(x, y)$, $\frac{dy}{dt} \equiv Q(x)$ for notational convenience.

It is well-known that for differentiable $F(x)$ and continuous $g(x)$ and $\psi(y)$ the following result holds true:

Lemma A.1. *For any periodic orbit Γ with $x = x_\gamma(t)$, $y = y_\gamma(t)$, periodic functions satisfying (2.1) with $F(x)$ continuously differentiable, continuous $g(x)$ and $\psi(y)$:*

$$\iint_{int(\Gamma)} f(x) dx dy = 0. \tag{A.1}$$

This lemma follows in a straightforward way from the application of Green's theorem:

$$\iint_{int(\Gamma)} f(x) dx dy = \iint_{int(\Gamma)} div \begin{pmatrix} P(x, y) \\ Q(x) \end{pmatrix} dx dy = \oint_\Gamma -Q(x) dx + P(x, y) dy.$$

The integrand of the last expression vanishes because by definition a solution Γ of system (2.1) is tangent to $\begin{pmatrix} dx \\ dy \end{pmatrix} = \begin{pmatrix} P(x, y) \\ Q(x) \end{pmatrix}$:

$$-Q(x)dx + P(x, y)dy = \left\langle \begin{pmatrix} -Q(x) \\ P(x, y) \end{pmatrix}, \begin{pmatrix} dx \\ dy \end{pmatrix} \right\rangle = \left\langle \begin{pmatrix} -Q(x) \\ P(x, y) \end{pmatrix}, \begin{pmatrix} P(x, y) \\ Q(x) \end{pmatrix} \right\rangle = 0.$$

For notational convenience we assumed that the periodic orbit is oriented counter-clockwise as we will continue to do in the following.

Next we will consider the case where the function $F(x)$ is a continuous, piecewise differentiable function, i.e. differentiable on intervals (x_-, x_f^1), (x_f^1, x_f^2), ..., (x_f^n, x_+), continuous at the points $x_f^1, x_f^2, ...x_f^n$ with finite jumps in the derivative $F'(x) \equiv f(x)$, the divergence of the vector field $\begin{pmatrix} P(x, y) \\ Q(x) \end{pmatrix}$ defined by (2.1), i.e. we consider the case of a piecewise-continuous $f(x)$. In [35] it was shown that piecewise differentiable functions of this type are Lipschitz continuous and that uniqueness of the solutions to (2.1) is guaranteed for all $x \in (x_-, x_+)$, $y \in (y_-, y_+)$.

We would like to prove that even for this case the lemma holds true. The problem arises from the fact that Green's theorem requires the functions to be differentiable. In our case we have a problem at the vertical lines $x = x_f^1, x = x_f^2, ...x = x_f^n$ intersecting the interior of the periodic orbit. If the periodic orbit does not intersect all of these vertical lines, we just omit those vertical

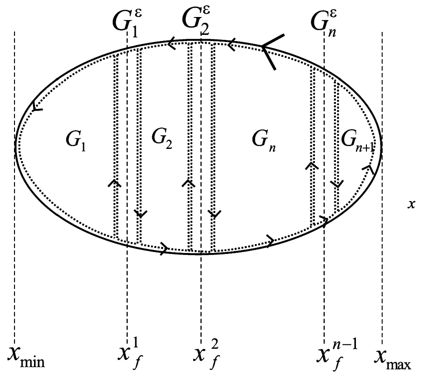

Fig. A.1. Division of a cycle into parts covering ϵ-neighborhoods of discontinuity points of $f(x)$.

lines from the rest of the discussion. Those non-intersecting lines have no impact on the integral over the interior of the periodic orbit.

We would like to apply Green's theorem for some parts of the area integral. In order to achieve this we apply the standard technique used in complex function theory and rewrite the periodic orbit Γ as a combination of appropriately chosen closed curves.

Denote by x_{min} and x_{max} the minimum and maximum x-value of the periodic orbit. We define a closed curve G_1 by joining Γ as defined on the interval $x_{min} \leq x < x_f^1 - \epsilon$ by the vertical line $x = x_f^1 - \epsilon$ and by introducing an upward orientation on this vertical line to make it a closed curve with counter-clockwise orientation.

Next we define the region G_1^ϵ, formed by $x_f^1 - \epsilon < x < x_f^1 + \epsilon$ joined by Γ at both ends of the interval. Continuing in this way, we can construct a set of counter-clockwise oriented closed curves $G_1,\ G_2, \ldots\ G_{n+1}$ which lie in the part where $F(x)$ is differentiable and a set G_1^ϵ, G_2^ϵ,... G_n^ϵ of open regions, each containing a line of discontinuity where $F(x)$ is continuous but not differentiable with a finite jump in the derivative $f(x)$. See Fig. A.1.

The original area integral can be written as the sum over the interiors of the closed curves we just defined:

$$\iint\limits_{int(\Gamma)} f(x)dxdy = \sum_{i=1}^{n+1} \iint\limits_{int(G_i)} f(x)dxdy + \sum_{i=1}^{n} \iint\limits_{int(G_i^\epsilon)} f(x)dxdy.$$

The important observation is that we can apply Green's theorem to the area integral over the interiors of the curves G_i because the integrand $f(x)$ is continuous there by construction. Since the normal of the vector field is still perpendicular to the parts of the curves G_i corresponding to Γ applying Green's theorem only gives a contribution of the line integral along the vertical lines $x = x_f^1 - \epsilon$, $x = x_f^1 + \epsilon$, $x = x_f^2 - \epsilon$, $x = x_f^2 + \epsilon$,...$x = x_f^n - \epsilon$, $x = x_f^n + \epsilon$:

$$\sum_{i=1}^{n+1} \iint\limits_{int(G_i)} f(x)dxdy =$$

$$\sum_{i=1}^{n}\int\limits_{y_i^{min}(-\epsilon)}^{y_i^{max}(-\epsilon)}(F(x_f^i-\epsilon)-\psi(y))dy-\sum_{i=1}^{n}\int\limits_{y_i^{min}(+\epsilon)}^{y_i^{max}(+\epsilon)}(F(x_f^i+\epsilon)-\psi(y))dy.$$

The minus-sign appears because of the opposite orientation along the vertical lines.

From the continuity of $F(x)$ and the continuity of the solution Γ (i.e. expressions like $y_i^{min}(-\epsilon)-y_i^{min}(+\epsilon)$ are of order ϵ) we can estimate the integral:

$$\sum_{i=1}^{n+1}\iint\limits_{int(G_i)} f(x)dxdy=$$

$$\sum_{i=1}^{n}\int\limits_{y_i^{min}(-\epsilon)}^{y_i^{max}(-\epsilon)}(F(x_f^i-\epsilon)-\psi(y))dy-\int\limits_{y_i^{min}(+\epsilon)}^{y_i^{max}(+\epsilon)}(F(x_f^i+\epsilon)-\psi(y))dy=$$

$$\sum_{i=1}^{n}F(x_f^i-\epsilon)(y_i^{max}(-\epsilon)-y_i^{min}(-\epsilon))-F(x_f^i+\epsilon)(y_i^{max}(+\epsilon)-y_i^{min}(+\epsilon))+$$

$$-\Psi(y_i^{max}(-\epsilon))+\Psi(y_i^{min}(-\epsilon))+\Psi(y_i^{max}(+\epsilon))-\Psi(y_i^{min}(+\epsilon)),$$

where $\Psi(y)\equiv\int\psi(y)dy$.
We rearrange the first part of the expression:

$$\sum_{i=1}^{n}[F(x_f^i-\epsilon)y_i^{max}(-\epsilon)-F(x_f^i+\epsilon)y_i^{max}(+\epsilon)]+[-F(x_f^i-\epsilon)y_i^{min}(-\epsilon)+F(x_f^i+\epsilon)y_i^{min}(+\epsilon)]$$

$$\frac{1}{2}(y_i^{max}(-\epsilon)-y_i^{min}(-\epsilon))^2-\frac{1}{2}(y_i^{max}(+\epsilon)-y_i^{min}(+\epsilon))^2.$$

Take in the above expression for example the term $F(x_f^i-\epsilon)y_i^{max}(-\epsilon)-F(x_f^i+\epsilon)y_i^{max}(+\epsilon)$. This term can rewritten as (taking absolute values anticipating the following calculation):

$$|F(x_f^i-\epsilon)y_i^{max}(-\epsilon)-F(x_f^i+\epsilon)(y_i^{max}(+\epsilon)|=$$

$$\frac{1}{2}|(F(x_f^i-\epsilon)+F(x_f^i+\epsilon))(y_i^{max}(-\epsilon)-y_i^{max}(+\epsilon))+$$

$$(F(x_f^i-\epsilon)-F(x_f^i+\epsilon))(y_i^{max}(-\epsilon)+y_i^{max}(+\epsilon))|<C_1\epsilon.$$

For the other term we obtain a similar estimate using the continuity of $F(x)$ and $y(x)$ (the solution to the differential equation).
For the remaining term we easily get:

$$|-\Psi(y_i^{max}(-\epsilon))+\Psi(y_i^{min}(-\epsilon))+\Psi(y_i^{max}(+\epsilon))-\Psi(y_i^{min}(+\epsilon))|<C_2\epsilon,$$

where we used that the continuity of $\psi(y)$ implies the continuity of its integral $\Psi(y)$. Combining all estimates we finally get:

$$|\sum_{i=1}^{n+1} \iint_{int(G_i)} f(x)dxdy| =$$

$$|\sum_{i=1}^{n} \int_{y_i^{min}(-\epsilon)}^{y_i^{max}(-\epsilon)} (F(x_f^i - \epsilon) - \psi(y))dy - \sum_{i=1}^{n} \int_{y_i^{min}(+\epsilon)}^{y_i^{max}(+\epsilon)} (F(x_f^i + \epsilon) - \psi(y))dy| < K_1\epsilon.$$

Next we consider the integrals over the interiors of G_i^ϵ. We rectangularize the area of integration by writing $y_i^{min} \equiv min(y(x))$ and $y_i^{max} \equiv max(y(x))$ on the interval $[x_f^i - \epsilon, x_f^i + \epsilon]$. We get:

$$|\sum_{i=1}^{n} \iint_{int(G_i^\epsilon)} f(x)dxdy| <$$

$$\sum_{i=1}^{n} \iint_{int(G_i^\epsilon)} |f(x)|dxdy <$$

$$\sum_{i=1}^{n} \int_{y_i^{min}}^{y_i^{max}} \int_{x_f^i-\epsilon}^{x_f^i+\epsilon} |f(x)|dxdy.$$

Since we assume that $f(x)$ makes at worst a finite jump at the points of discontinuity, we know it is bounded: $|f(x)| < c_i$ around each discontinuity point. With this the estimate becomes:

$$\sum_{i=1}^{n} \int_{y_i^{min}}^{y_i^{max}} \int_{x_f^i-\epsilon}^{x_f^i+\epsilon} |f(x)|dxdy <$$

$$\sum_{i=1}^{n} \int_{y_i^{min}}^{y_i^{max}} \int_{x_f^i-\epsilon}^{x_f^i+\epsilon} c_i dxdy =$$

$$\sum_{i=1}^{n} (y_i^{max} - y_i^{min})(x_f^i + \epsilon - x_f^i + \epsilon)c_i = K_2\epsilon.$$

It implies that the original integral over the interior of the periodic orbit can be estimated as:

$$|\iint_{int(\Gamma)} f(x)dxdy| < (K_1 + K_2)\epsilon.$$

Since ϵ can be chosen arbitrarily small, it follows that

$$\iint\limits_{int(\Gamma)} f(x)dxdy = 0,$$

as we set out to prove.

The consequences are that many theorems about non-existence of limit cycles in Liénard systems can be extended in a straightforward way to the piecewise differentiable case, because these theorems are based on the fact that the integral of the divergence $f(x)$ over the interior of a periodic orbit is equal to zero.

Appendix B. The characteristic exponent for piecewise differentiable systems

This appendix contains the proof of Lemma 3.4.

Proof. Consider the following planar autonomous system of ordinary differential equations:

$$\begin{aligned} \frac{dx(t)}{dt} &= P(x,y), \\ \frac{dy(t)}{dt} &= Q(x,y). \end{aligned} \tag{B.1}$$

Later we will consider the case where $P(x, y)$ and $Q(x, y)$ are continuous, piecewise differentiable functions in x, y with finite jumps in the derivatives at the points where the functions are not differentiable. We will assume that these points of discontinuity appear at isolated one-dimensional manifolds in the plane.

First we consider the well-known general case where $P(x, y)$ and $Q(x, y)$ are differentiable.

In [1] the following result was proved for the derivative of the succession function of (B.1) (chapter 28 auxiliary material, lemma 4). We consider (using their notation) two arcs without contact l_1 and l_2 parametrized by u and $\bar{u}$ through $x = g_1(u)$, $y = h_1(u)$ and $x = g_2(\bar{u})$, $y = h_2(\bar{u})$ respectively. We suppose that solutions on appropriately defined intervals for u start at l_1 and reach l_2 after finite time. Without loss of generality we may assume that each solution starts at l_1 at time $t = 0$. The time to reach l_2 from l_1 is written as $\chi(u)$ and the point where the solution reaches l_2 is written as $\bar{u} = \omega(u)$, referred to as the succession function. With this notation [1] proves:

Lemma B.1. *[1] The derivative of the correspondence function $\omega(u)$ can be written as:*

$$\omega'(u) = \frac{d\omega(u)}{du} = \frac{\Delta_1(u)}{\Delta_2(u)} e^{\int_0^{\chi(u)}[P'_x(\phi(t),\psi(t))+Q'_y(\phi(t),\psi(t))]dt}, \tag{B.2}$$

where

$$\Delta_1(u) = \begin{vmatrix} P(g_1(u), h_1(u)) & g'_1(u) \\ Q(g_1(u), h_1(u)) & h'_1(u) \end{vmatrix},$$

$$\Delta_2(u) = \begin{vmatrix} P(g_2(\omega(u)), h_2(\omega(u))) & g'_2(\omega(u)) \\ Q(g_2(\omega(u)), h_2(\omega(u))) & h'_2(\omega(u)) \end{vmatrix},$$

and $\phi(t)$, $\psi(t)$ are solutions to (B.1) with initial conditions $x = \phi(0) = g_1(u)$, $y = \psi(0) = h_1(u)$.

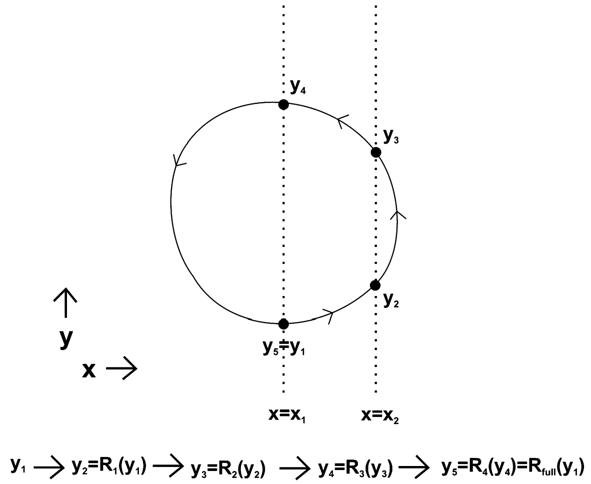

Fig. B.1. Example of dividing a periodic orbit into 4 parts, each of which lies in a region where the Liénard system is differentiable. $f(x)$ is continuous except at the points $x = x_1$ and $x = x_2$ in this example.

The important observation about the structure of the expression in the lemma is that the integral expression only depends on the path and its traversal time, not the actual parametrizations of the arcs without contact. These two arcs appear in the two determinants forming the quotient $\frac{\Delta_1(u)}{\Delta_2(u)}$.

In the following we will consider a special case of this general lemma, i.e. for the generalized Liénard system (2.1).

We will assume that the function $F(x)$ in (2.1) is a continuous, piecewise differentiable function, i.e. differentiable on intervals (x_-, x_f^1), (x_f^1, x_f^2), ..., (x_f^n, x_+), continuous at the points x_f^1, x_f^2, ..., x_f^n. At these isolated points the derivative $F'(x) \equiv f(x)$ (which is the divergence of the vector field defined by (2.1)) has finite jumps, i.e. we consider the case of a piecewise-continuous $f(x)$. In [35] it was shown that piecewise differentiable functions of this type are Lipschitz continuous implying that uniqueness of the solutions to (2.1) is guaranteed for all $x \in (x_-, x_+)$, $y \in (y_-, y_+)$ if $F(x)$ and $g(x)$ are piecewise differentiable functions.

In Fig. B.1 a simple situation is shown with a periodic solution in the case of two discontinuity points at $x = x_1$ and $x = x_2$. The idea for finding an expression for the derivative of the Poincaré map for the periodic solution is to split the curve into pieces defined on open intervals for x where (2.1) is differentiable.

Consider the subset of x-values of $x_f^1, x_f^2, ...x_f^n$ corresponding to those vertical lines $x = x_i$ having an intersection point with a periodic solution. Denote this set by S with ordered x-values $x_s^1, ...x_s^j$.

Consider a point on $x = x_s^1$, with y-coordinate y_1 where a periodic orbit intersects the first vertical line corresponding to set S. For convenience of the discussion we assume that this point is the lower point of intersection (since the periodic orbit will intersect the vertical line in two points $y = y_1^*$, $y = y_2^*$, with $y_1^* < y_2^*$, we choose as the starting point $y_1 = y_1^*$). The lines $x = x_s^i$ in set S are lines without contact for the periodic orbit and will serve as the arcs without contact used in Lemma B.1. The solution starting at $x = x_s^1$, $y = y_1$ will have consecutive intersection points at $y_1, y_2, .., y_j$ on the vertical lines $x_s^1, ...x_s^j$ while traversing the lower part of the periodic orbit. After it has reached the last vertical line, it will intersect the same line again at the upper part of the periodic orbit at $y = y_{j+1}$. From there on it will intersect the set $x_s^1, ...x_s^j$ for a second time traversing it in a leftward direction along the upper part of the periodic orbit until it reaches the first vertical line x_s^1 at some point y_{2j}. Finally the orbit starting at (x_s^1, y_{2j}) returns to the original line segment $x = x_s^1$ at some point $y_{2j+1} < y_{2j}$ defining a return mapping $y_{2j+1} = R_{full}(y_1)$. We define the Poincaré mapping through $Z(y_1) \equiv R_{full}(y_1) - y_1$. For a periodic orbit this function will have a zero. Here we adopted the convention that the periodic orbit is traversed in a counter-clockwise direction.

The full Poincaré mapping $Z(y_1)$ consists of $2j$ composite succession functions. Each successsion function is defined on two arcs of the form $x = c_1$, $x = c_2$, defined by the mapping between the two y-coordinates. In Lemma B.1 this corresponds to the following choice of functions: $x = g_1(u) \equiv x_s^i$, $y = h_1(u) = u$ and $x = g_2(\bar{u}) \equiv x_s^{i+1}$, $y = h_2(\bar{u}) = \bar{u}$. The chain of consecutive mappings can therefore be written as: $Z(y_1) = y_{2j+1} - y_1 = R_{2j}(y_{2j}) - y_1 = R_{2j}(R_{2j-1}(y_{2j-1})) - y_1 = R_{2j}(R_{2j-1}(....R_1(y_1))) - y_1 \equiv R_{full}(y_1) - y_1$.

We are interested in the derivative of this mapping with respect to the original parameter y_1. Using the derivative of composite function we get:

$$\frac{dZ(y_1)}{dy_1} = \frac{dR_{full}(y_1)}{dy_1} - 1 = \frac{dy_{2j+1}}{dy_1} - 1 = \frac{dR_{2j}(y_{2j})}{dy_{2j}} \frac{dR_{2j-1}(y_{2j-1})}{dy_{2j-1}} ... \frac{dR_1(y_1)}{dy_1} - 1. \tag{B.3}$$

For each factor we can apply Lemma B.1. Consider a factor of the type $\frac{dR_i(y_i)}{dy_i}$ which represents the derivative of the succession function between two arcs with y-coordinates y_i and y_{i+1} respectively. According to Lemma B.1 we have:

$$\frac{dR_i(y_i)}{dy_i} = \frac{F(x_s^i) - \psi(y_i)}{F(x_s^{i+1}) - \psi(y_{i+1})} e^{\int_0^{\chi_i(x_s^i)} f(x(t))dt}, \tag{B.4}$$

where $\chi_i(x_s^i)$ is the time to traverse the i_{th}-arc. The two determinants in $\frac{\Delta_1(u)}{\Delta_2(u)}$ of Lemma B.1 simplify because $g_1'(u) = 0$ and $g_2'(\omega(u)) = 0$.

Applying (B.4) to all factors in (B.3) we get:

$$\frac{dR_{full}(y_1)}{dy_1} = \frac{F(x_s^1) - \psi(y_1)}{F(x_s^{2j+1}) - \psi(y_{2j+1})} e^{\int_0^{\chi_1(x_s^1)} f(x(t))dt} e^{\int_0^{\chi_2(x_s^2)} f(x(t))dt} ... e^{\int_0^{\chi_{2j}(x_s^{2j})} f(x(t))dt}.$$

Here we used the notation $x_s^{j+1} = x_s^j$, $x_s^{j+2} = x_s^{j-1}$, ..., $x_s^{2j} = x_s^1$, for the part of the curve traversing from right to left.

Since $x_s^{2j+1} = x_s^1$ and $y_{2j+1} = y_1$ for a periodic orbit we get that:

$$\frac{dZ(y_1)}{dy_1} = \frac{dR_{full}(y_1)}{dy_1} - 1 = e^{\int_0^T f(x(t))dt} - 1.$$

where T is the time it takes to traverse one full cycle of the periodic orbit. This is exactly the well-known formula which is valid for differentiable $F(x)$ as typically used in the literature for Liénard equations.

For a periodic orbit it implies that the sign of the derivative of the Poincaré mapping is determined by the sign of the contour integral of $f(x)$ along the periodic orbit, i.e. the so-called characteristic exponent determining the stability of a periodic solution is given by:

$$\oint_{\Gamma} f(x(t))dt.$$

It follows that the conclusions in Liénard systems regarding uniqueness of limit cycles and non-existence of limit cycles still hold for a piecewise differentiable $F(x)$, because those theorems typically use the fact that the sign of $\int_0^T f(x(t))dt$ determines the stability of a limit cycle in a Liénard system. □

References

[1] A.A. Andronov, et al., Theory of Bifurcation of Dynamical Systems on the Plane, translated by John Wiley and Sons, New York, 1973.

[2] J. Cheng, R. Zhang, The qualitative analysis of two species predator-prey model with Holling type III functional response, Appl. Math. Mech. 7 (1986) 77–86.

[3] G. Dai, M. Tang, Coexistence region and global dynamics of a harvested predator-prey system, SIAM J. Appl. Math. 58 (1998) 193–210.

[4] D.M. Dubois, P.L. Closset, Patchiness in primary and secondary production in the Southern Bight: a mathematical theory, in: G. Persoone, E. Jaspers (Eds.), Proceedings of the 10th European Symposium on Marine Biology, Universa Press, Ostend, 1976, pp. 211–229.

[5] P. De Maesschalck, F. Dumortier, Canard solutions at non-generic turning points, Trans. Am. Math. Soc. 358 (5) (2006) 2291–2334.

[6] P. De Maesschalck, F. Dumortier, Canard cycles in the presence of slow dynamics with singularities, Proc. R. Soc. Edinb. A 138 (2) (2008) 265–299.

[7] P. De Maesschalck, F. Dumortier, Classical Liénard equation of degree $n \geq 6$ can have $[\frac{n-1}{2}] + 2$ limit cycles, J. Differ. Equ. 250 (2011) 2162–2176.

[8] P. De Maesschalck, F. Dumortier, R. Roussarie, Cyclicity of common slow-fast cycles, Indag. Math. (N. S.) 22 (2011) 165–206.

[9] P. De Maesschalck, F. Dumortier, R. Roussarie, Canard cycle transition at a slow-fast passsage through a jump point, C. R. Math. Acad. Sci. Paris 352 (4) (2014) 317–320.

[10] F. Dumortier, R. Roussarie, Canard cycles and center manifolds, Mem. Am. Math. Soc. 121 (577) (1996).

[11] F. Dumortier, R. Roussarie, Multiple canard cycles in generalized Liénard equations, J. Differ. Equ. 174 (1) (2001) 1–29.

[12] H.I. Freedman, Deterministic Mathematical Models in Population Ecology, Marcel Dekker, New York, 1980.

[13] H.I. Freedman, G.S.K. Wolkowicz, Predator-prey systems with group defence: the paradox of enrichment revisited, Bull. Math. Biol. 48 (1986) 493–508.

[14] E. Freire, E. Ponce, F. Rodrigo, F. Torres, Bifurcation sets of continuous piecewise linear systems with two zones, Int. J. Bifurc. Chaos Appl. Sci. Eng. 8 (1998) 2073–2097.

[15] G.F. Gause, The Struggle for Existence, Williams and Wilkins, Baltimore, 1934.

[16] C.S. Holling, The components of predation as revealed by a study of small-mammal predation of the European pine sawfly, Can. Entomol. 91 (1959) 293–320.

[17] C.S. Holling, The functional response of predators to prey density and its role in mimicry and population regulation, Mem. Entomol. Soc. Can. 45 (1965) 3–60.

[18] J. Huang, S. Ruan, J. Song, Bifurcations in a predator-prey system of Leslie type with generalized Holling type III functional response, J. Differ. Equ. 257 (2014) 1721–1752.

[19] J. Huang, D. Xiao, Analyses of bifurcations and stability in a predator-prey system with Holling type-IV functional response, Acta Math. Appl. Sin., English Ser. 20 (2004) 167–178.

[20] J.M. Jeschke, M. Kopp, R. Tollrian, Predator functional responses: discriminating between handling and digesting prey, Ecol. Monogr. 72 (1) (2002) 95–112.

[21] P.K. Jha, S. Ghorai, Stability of prey-predator model with Holling type response function and selective harvesting, J. Appl. Comput. Math. 6 (3) (2017) 1–7.

[22] N. Kazarinov, P. van der Driessche, A model predator-prey system with functional response, Math. Biosci. 39 (1978) 125–134.

[23] K. Yang, H.I. Freedman, Uniqueness of limit cycles in Gause type models of predator-prey systems, Math. Biosci. 88 (1988) 67–84.

[24] R.E. Kooij, A. Zegeling, Qualitative properties of two-dimensional predator-prey systems, J. Nonlinear Anal. 29 (6) (1997) 693–715.
[25] R.E. Kooij, A. Zegeling, Predator-prey models with non-analytical functional response, Chaos Solitons Fractals 123 (2019) 163–172.
[26] C. Li, K. Lu, Slow divergence integral and its application to classical Liénard equations of degree 5, J. Differ. Equ. 257 (2014) 4437–4469.
[27] X.Y. Li, W.D. Wang, Qualitative analysis of predator-prey system with Holling type I functional response, J. South China Normal Univ. Natur. Sci. Ed. 29 (2004) 712–717.
[28] C. Li, H. Zhu, Canard cycles for predator-prey systems with Holling types of functional response, J. Differ. Equ. 254 (2013) 879–910.
[29] N. Liu, Limit cycles for a predator-prey model with functional response of Holling type I, Chin. Ann. Math. 9a (4) (1988) 421–427 [in Chinese].
[30] B. Liu, Y. Zhang, L. Chen, Dynamics complexities of a Holling I predator-prey model concerning periodic biological and chemical control, Chaos Solitons Fractals 22 (2004) 123–134.
[31] J. Llibre, E. Ponce, F. Torres, On the existence and uniqueness of limit cycles in Liénard differential equations allowing discontinuities, Nonlinearity 21 (2008) 2121–2142.
[32] Y. Ren, L. Han, The predator prey model with two limit cycles, Acta Math. Appl. Sin. (English Ser.) 5 (1989) 30–32.
[33] M.L. Rosenzweig, R.H. McArthur, Graphical representation and stability conditions of predator-prey interactions, Am. Nat. 47 (1963) 209–223.
[34] F. Rothe, D.S. Shafer, Multiple bifurcation in a predator-prey system with nonmonotonic predator response, Proc. R. Soc. Edinb. A 120 (1992) 313–347.
[35] S. Scholtes, Introduction to Piecewise Differentiable Functions, Springer, New York, 2012, pp. 91–111.
[36] G. Seo, M. Kot, A comparison of two predator-prey models with Holling's type I functional response, Math. Biosci. 212 (2008) 161–179.
[37] G. Seo, D.L. DeAngelis, A predator-prey model with a Holling type I functional response including a predator mutual interference, J. Nonlinear Sci. 21 (6) (2011) 811–833.
[38] D. Xiao, H. Zhu, Multiple focus and Hopf bifurcations in a predator-prey system with nonmonotonic functional response, SIAM J. Appl. Math. 66 (2006) 802–819.
[39] Z. Zhang, et al., Qualitative Theory of Differential Equations, American Math. Soc., 1992, 461 pages.
[40] Y. Zhang, Z. Xu, B. Liu, Dynamic analysis of a Holling I predator-prey system with mutual interference concerning pest control, J. Biol. Syst. 13 (2005) 45–58.
[41] Y. Zhou, C. Wang, D. Blackmore, The uniqueness of limit cycles for Liénard system, J. Math. Anal. Appl. 304 (2) (2005) 473–489.
[42] H. Zhu, S.A. Campbell, G.S.K. Wolkowicz, Bifurcation analysis of a predator-prey system with nonmonotonic function response, SIAM J. Appl. Math. 63 (2002) 636–682.